PROBABILISTIC SEISMIC HAZARD MAPS FOR ADANA PROVINCE IN TURKEY

Tuba Eroğlu Azak [a] and Senem Tekin [b]*

[a] Akdeniz University, Department of Civil Engineering
[b] Çukurova University, Department of Geological Engineering
*E-mail address: tubaeroglu@akdeniz.edu.tr

Abstract

Turkey is located in a highly seismic region, where $M_w > 6.5$ earthquakes take place in every 10 year. According to the seismic zonation map of Turkey, approximately 42 % of the Turkish territory is located in the most seismic prone zone, known as Zone I. The other seismic zones are termed as Zone II, III and IV from the second severe to the least severe one. In this paper, we investigated the seismicity of Adana Province that is situated on four different seismic zones (i.e. Zone I to IV). Accordingly, we developed probabilistic seismic hazard maps of Adana for 475 year return period for stiff and soft site conditions. The probabilistic seismic hazard maps are presented in terms of PGA. The comparative maps indicate remarkable differences between proposed PGA values and the current design PGA values provided by the seismic zonation map and Turkish Earthquake Code.

Keywords: Probabilistic seismic hazard map, seismic hazard in Adana, seismic hazard assessment, PGA hazard map

1. Introduction

Turkey is one of the most seismic prone areas in the world. In the last century, more than a hundred earthquakes have occurred with catastrophic consequences at different levels. Among these, earthquakes occurred at the last decade of 20th century have served as a landmark for better understanding of seismic hazard and seismic risk. In particular, Kocaeli and Düzce earthquakes occurred one after the other in 1999 started renaissance in structural and earthquake engineering in Turkey. As these earthquakes caused large number of casualties and high socio-economic losses, North Anatolian Fault (NAF) and seismic hazard on southwestern part of Turkey have been the main focus of many studies. However, one needs consider that seismic hazard in Turkey is spread on a larger scale throughout the country. In this sense, proper estimation of seismic hazard in the entire seismic prone regions is the primary step of seismic risk mitigation studies in Turkey.

According to the seismic zonation map of Turkey, four seismic zones are defined within the Turkish territory. These zones are termed as Zone I, II, III and IV with respect to decreasing seismic hazard. There exists a final zone called as Zone IV that is regarded as hazard-free. In seismic design of most of the engineered buildings, Turkish seismic zonation map is the main input while estimating earthquake induced forces. Thus, reliable estimation of seismic hazard is of prime importance as seismic performance of buildings are directly linked to the seismic threats.

In this paper, we investigated seismic hazard of Adana Province that is located in the southern part of Turkey. According to the seismic zonation map, Adana province is situated on four different seismic zones. In this respect, Adana is an interesting case in terms of seismic hazard and risk assessment. In Adana two destructive earthquakes have occurred in the instrumental period (approximately the last 100 years). The Ceyhan-Misis earthquake with a magnitude of

M_s 6.0 hit the Adana in 1945 and resulted in heavy damage to 650 buildings and 10 casualties. More recently, Ceyhan earthquake with a magnitude of M_w 6.2 killed 146 people, resulted in heavy damage to 11,000 buildings and destroyed 1,300 buildings [1].

The seismic hazard assessment in Adana is conducted on the basis of probabilistic seismic hazard analysis (PSHA) that quantifies the exceedance probabilities at various levels of a given ground-motion parameter for a given future time period. The seismicity in Adana is modeled by area source models. As the final product, seismic hazard maps of Adana are proposed in terms of Peak Ground Acceleration (PGA) at 475 year return period. The site conditions are chosen as NEHRP C and NEHRP D that are considered to reflect the most common site profiles of the engineered buildings in Turkey. As the entire body of this study is based on seismic hazard assessment in Adana by utilizing the updated earthquake catalogs and revised fault map, the main goal of this paper is to present up-to-date seismic hazard maps for the area of interest. Accordingly, the proposed seismic hazard maps in terms of PGA are compared with the ones provided by the seismic zonation map and Turkish Earthquake Code (TEC, 2007) [2]. The presented results are believed to stimulate further discussions on seismic hazard in Adana and to be helpful for seismic hazard assessment studies in the area.

2. Methodology

The aim of probabilistic seismic hazard assessment (PSHA) is to determine the probability that the selected ground motion intensity measure (e.g. PGA, PSA, PSV) will exceed a certain threshold in a given period. In order to execute PSHA, Poisson model is assumed to be valid for earthquake occurrences. According to the Poisson process, three basic assumptions are used that can be listed as:
- Earthquake occurrences are spatially independent
- Earthquake occurrences are temporally independent
- The probability that two earthquakes occur at the same location and at the same time is zero

While conducting PSHA, all potential seismic sources in the vicinity of the site of interest are taken into account. These sources must be represented by reliable models that are able reflect the characteristics of seismic sources and uncertainties related with earthquake process. This task can only be accomplished by proper investigation on seismotectonic regimes, geological formations and seismic data for the area of interest. In this study, we modeled the seismicity of Adana by making use of area source zones as they provide data reduction in seismic hazard analysis [3]. An area source zone is defined as a seismically homogenous zone, in which every point within the region has an equal probability to be the epicenter of a future earthquake [4]. While determining the geometry as well as properties of area sources, we considered historical and recorded seismicity together with a comprehensive knowledge that is based on structural geology, neotectonic and seismotectonic structure of the area of interest. Accordingly we established a total of 14 area source zones. Truncated exponential distribution is applied to formulate the magnitude recurrence relationship of the area source models. The activity rates and recurrence parameters are estimated by making use of historical and instrumental seismicity. As the earthquake occurrences are considered to verify Poisson process, the fore and aftershocks are removed from the earthquake catalogs before estimating the magnitude recurrence relationships.

The other important component of PSHA is the ground motion prediction equations (GMPEs) that are utilized to relate ground motion parameters with earthquake characteristics. While

their number in the literature is abundant, GMPEs differ considerably due to inherent characteristics of the employed ground motion databases and selected functional forms. In this sense the selection of the appropriate GMPEs for the area of interest is of prime importance. In this paper, we utilized a total of six GMPEs that are considered to be compatible with earthquake characteristics in Turkey. Among the six GMPEs, three of them are utilized to model area sources related with active shallow crust earthquakes whereas the rest are employed for the inter slab earthquake occurrences in subduction zones.

In order to conduct PSHA, EZ-Frisk software is utilized. Multi-site PSHA is performed at 249 sites that are located on a 0.1^0x0.1^0 grid. The iso-acceleration hazard map coordinates are calculated by bilinear interpolation between the grid points. The detailed information on each component of the study can be found in the subsequent parts of the study.

3. Geology of Adana

The study area is located in Taurus zone between Ecemiş Fault and Yumurtalık Fault. The Adana province and its surroundings, which are within the boundaries of this study area, include various tectonically tectonostratigraphic units that have significant differences in terms of distinguished stratigraphy, structure and lithology [5] (Figure 1). Bolkar Mountains include olistostrome featured rock as well as carbonate and clastic rocks precipitated from Devonian-Lower Tertiary period (There are acidic, basic and ultrabasic rocks, tuffs and serpentinites representing different facies and environments ranging from continental slope and oceanic rocks to shelf-type rocks precipitated from the period of Triassic-Senonian located in the Bozkır Mountains. Aladağ Mountains include shelf-type carbonate and clastic rocks representing the period of Devonian-Cretaceous. Geyik Mountains have carbonate and clastic rocks of Early-Cambrian Tertiary period. Görbiyes Mountains include carbonate sequence, olistholites and olistostromal formations representing possibly the period of Jurassic-Late Cretaceous. Görbiyes Mountains shows low-grade metamorphism. The range of Keban-Malatya is mostly represented by platform type meta-clastic and meta-carbonate rocks that are within the Upper Paleozoic-Lower Cretaceous age period. Misis-Andırın Mountains present the mélange featured volcano sediment facies characteristics, deposited within the time period of Cretaceous-Tertiary. The cover units consist of shallow marine and pelagic (deeper sea level > 1000 m) deposits from the period of Tertiary-Quaternary [6].
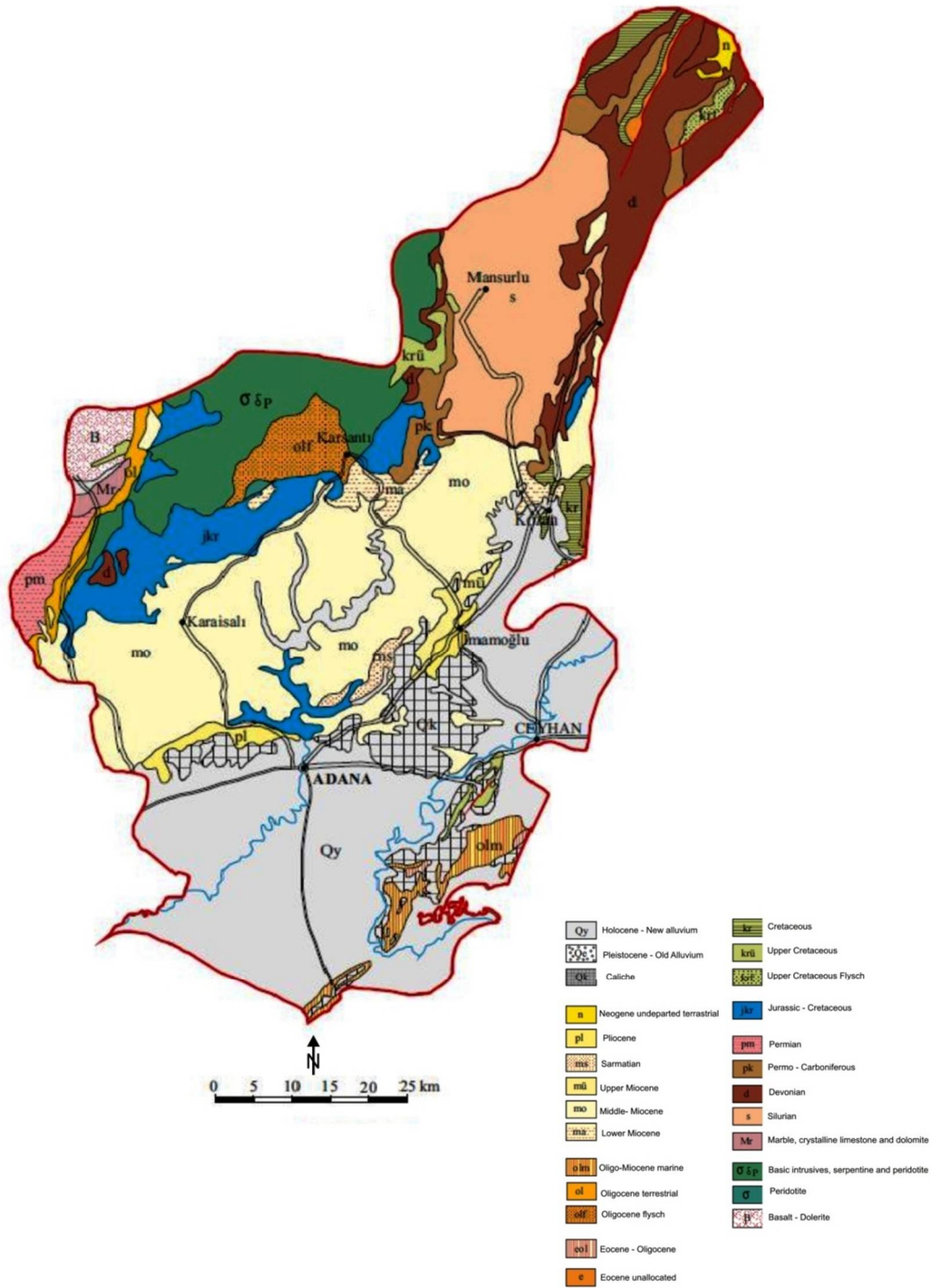
Figure 1. Geology of Adana Province by Usta [6]

4. Seismic Sources

4.1. Seismotectonics of Adana

The seismotectonic structure of the eastern Mediterranean region, where Adana is located, can be explained by the relative motion between Arabian, African and Euroasian plates. Due to collusion between Arabian and Euroasian plates, the Anatolian block is forced to move to the west towards to the Eastern Mediterranean ridge of African Plate [7]. This movement formed

106

the major neotectonic structures in Turkey and surrounding area that can be listed as dextral North Anatolian Fault Zone (NAFZ), sinistral East Anatolian Fault Zones (EAFZ) and Dead Sea Fault Zone (DSFZ) and Hellenic-Cyprus subduction zones [8].

Adana, located in the southern part of Turkey, is surrounded by EAFZ in the east, Central Anatolian Fault Zone (CAFZ) in the west and Cyprus Arc in the south. These structures constitute the major seismotectonic sources around the study area as depicted in Figure 2. More detailed plot of the active faults around Adana can be found in Figure 3. According to the current active fault map, there exist several faults near to the study area. Among them, the southern strand of EAFZ formed by Amanos and Pazarcık segments located to the east of Adana can be considered as the most active ones due to their slip rates. Sürgü, Çardak, Savrun, Çokak and Misis segments that constitute the northern strand of EAFZ accommodate lower slip rates compared to the southern strand [9]. Toprakkale Fault is another branch of EAFZ that splits from the northern strand around the west end of Sarız Fault. The seismicity of the area is also controlled by Sarız Fault and Ecemiş Faults that are located to the northern part of Adana. Another important structure in the surrounding area is the Dead Sea Fault Zone (DSFZ) that connects to the EAFZ and Cyprus Arc via Amik triple junction [9]. Cyprus Arc is formed due to subduction of African Plate beneath the Eurasian Plate. In this sense, Cyprus Arc is the main structure that produces deep earthquakes along the İskenderun Gulf. Düziçi-İskenderun Fault Zone located to the east of Adana comprises NW-striking normal faults between strands of the EAFZ. The fault zone delimits the Amanos Mountains in the west. Apart from these major structures, there are also minor faults such as Karataş and Yumurtalık Faults that extend parallel to the coast of the İskenderun Bay. It is worth to note here that some of the fault structures mentioned above were not identified in the previous version of the Turkish active fault map. This issue once again calls for importance of revision of the seismic hazard map of Turkey.
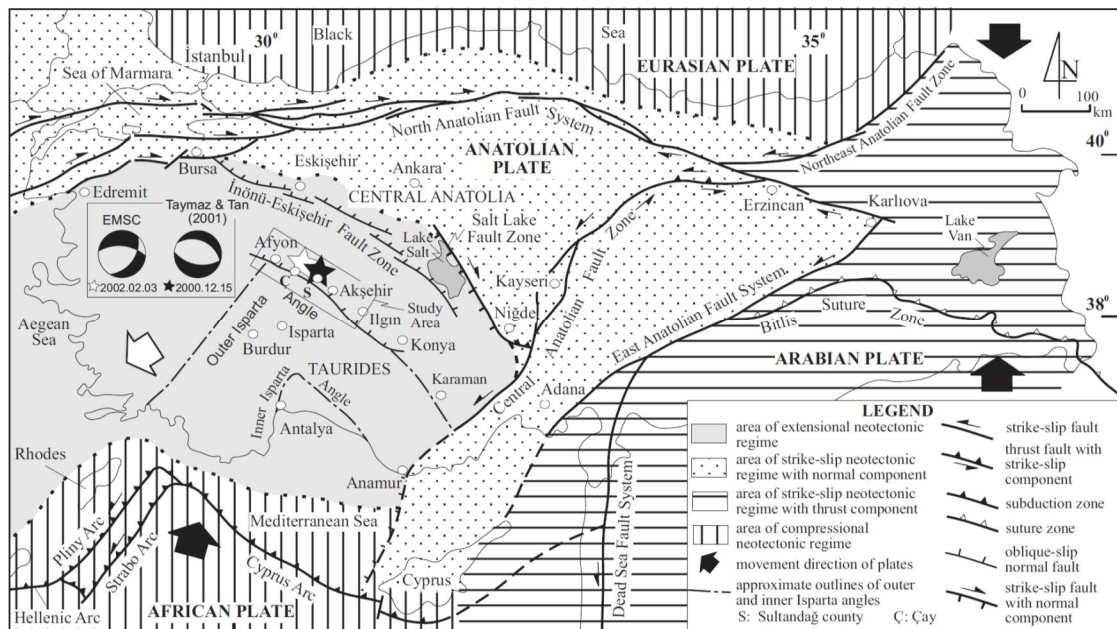

Figure 2. Simplified map of neotectonic structure for Turkey, Koçyiğit and Özacar [8]

Figure 3. Active fault map of Adana and its surroundings, (Emre et al. [10])

4.2. Historical Seismicity

The instrumental seismicity that only covers the earthquakes occurred from the beginning of the 20th century is often not sufficient when considering the long recurrence periods of big earthquakes. In this sense, the historical seismicity plays an important role in seismic hazard assessment while determining completeness of earthquake catalogs and calculating earthquake source models.

Figure 4 illustrates the epicenters of significant historical events with magnitudes M ≥ 6.5 in Adana and its surroundings [11]. As an immediate observation, one can infer that the seismic activity in the neighboring area of Adana is mainly concentrated along the zone formed by East Anatolian Fault and Dead Sea Fault Zones. According to the historical catalog the closest earthquake to the Adana Province occurred in 1513 with a magnitude of M_s 7.4. The historical records reveal that the seismic sources around Adana can produce big and destructive events. However, the historical seismicity itself does not provide enough yet reliable information to conduct seismic hazard analysis as historical catalogs are often related with the population around the site of interest and how the records are kept. In this sense, the historical evidences should be considered together with regional seismotectonics in order to reduce the level uncertainties in the seismic source characterization.
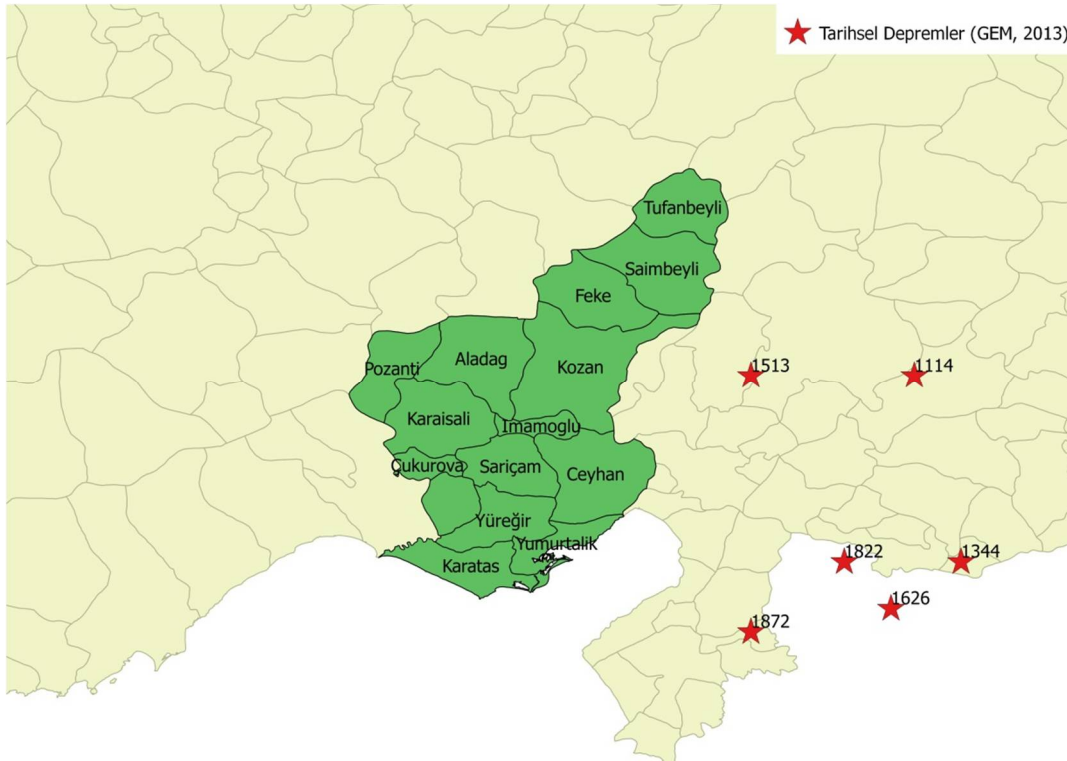
Figure 4. Historical earthquakes in the vicinity of Adana (GEM [11])

4.3. Area Source Models for Probabilistic Seismic Hazard Analysis

General idea that underpins the area source zonation is that within an area source the seismic characteristics must be kept as homogenous as possible provided that seismic data is sufficient to determine the area source parameters. Erdik et al. [4] indicate that the boundary between area sources should be drawn close to the highest concentration around the hard core of the most active one. Erdik et al. [4] also suggest that if there are sufficient number of events, the area source boundaries must be particularly related to the seismic data and supported by tectonic evidences whereas in case of insufficient number of events, the decision on the boundaries must be based on the most dominant tectonic structure. Woo [3] defines two types of tectonic boundaries. The first one is defined by the causal relationships between geological structures whereas the second one is designated by the faults that are historically inactive but showing recent activity.

Another prominent parameter on seismic zone zonation is the seismogenic depth. Due to different tectonic regimes in Turkey, the seismogenic depths differs from east to west and from north to south. For the earthquakes produced at the active shallow crust, the hypocentral depths attain values up to 30-40 km whereas interslab and interface earthquakes occurring at the subduction zones hypocentral depths reach very high values. In this sense, the seismogenic depth is another decisive factor in constructing the area source boundaries. Figure 5 presents the dispersion of hypocentral depths of the events from instrumental and historical catalog around Adana. As one infer from the figure, the hypocentral depths are particularly high in the Mediterranean Sea along Helenic and Cyprus Arcs where Arabian Plate is being subducted beneath Anatolian plate. Türkelli et al. [12] investigated the seismogenic depths in eastern Turkey. According to their findings, the seismogenic depths on EAFZ mainly concentrate in the 10-30 km depth range. Vanacore et al. [13] suggest a seismogenic depth of 20-30 km for the study area and state that the Moho thins to the South and West across Anatolia.
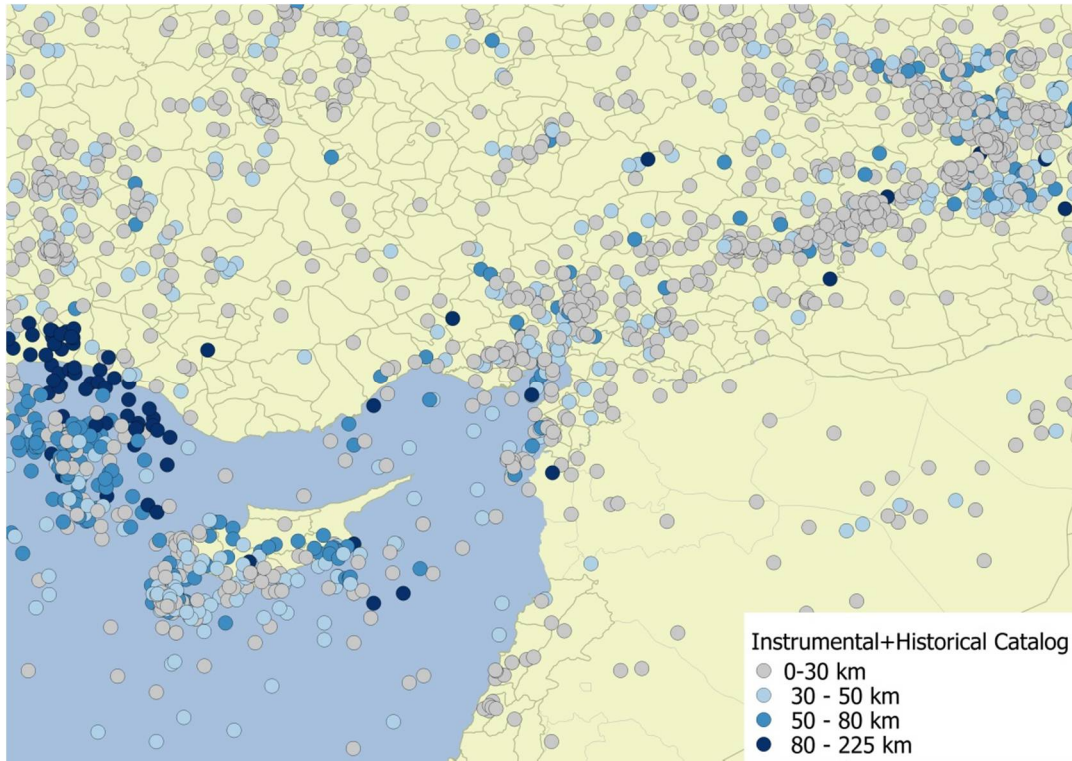
Figure 5. Scatter plot of hypocentral depths around the study area

In the light of the above discussion, the area source models are established in accordance with seismotectonic structure of Adana and its surroundings together with instrumental and historical seismicity data. A total 14 area sources generated considering a buffer zone with a width of 100 km around Adana Province. Figure 6 illustrates the area source models generated.

Figure 6. Area source models utilized in this study

5. Homogenous Catalog

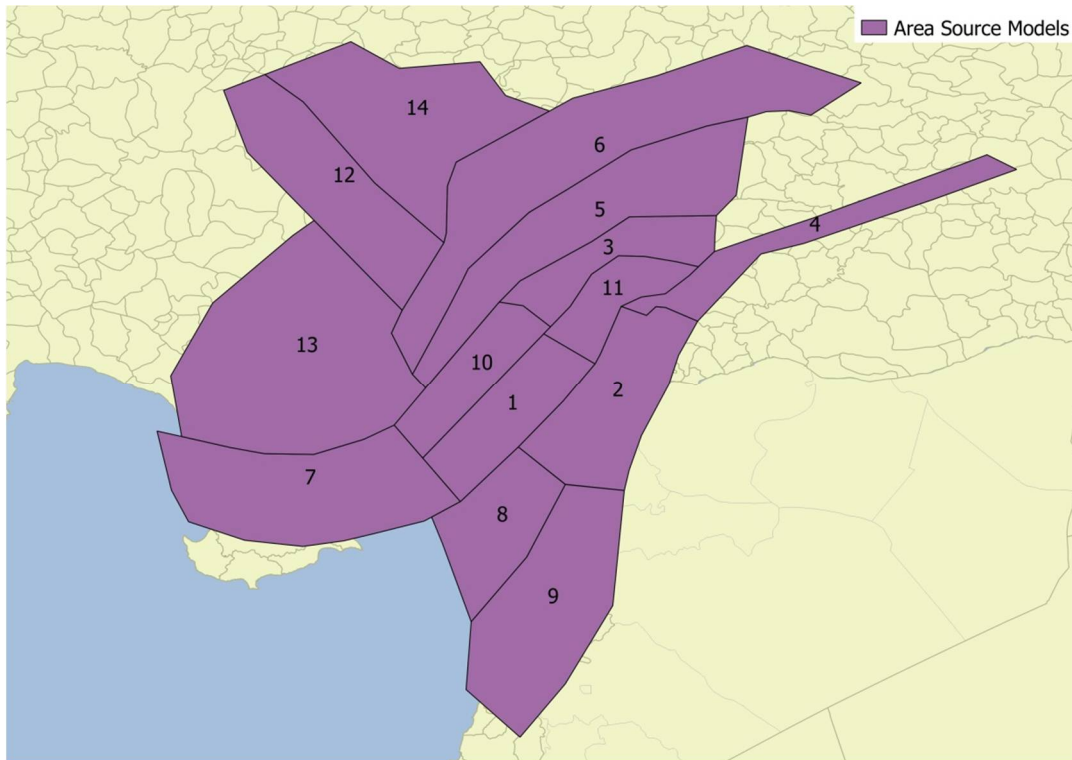The instrumental catalog we utilized in this study is the recent Turkish Earthquake Catalog [14] that is compiled by cooperation of Turkish Republic Prime Ministry Disaster and Emergency Management Presidency (AFAD), General Directorate of Mineral Research and Exploration (MTA) and Kandilli Observatory and Earthquake Research Institute (KOERI). The earthquake catalog is composed of 12674 earthquakes with magnitudes $M \geq 4.0$. Each earthquake in the catalog has a single unconverted magnitude value in one of the magnitude scales (e.g. M_s, m_b, M_d, M_l and M_w). However, for any calculation regarding earthquake catalogs, a common magnitude scale is essential. In order to obtain a homogenous catalog we made use of empirical relationships to covert different magnitude scales to M_w as it is the most reliable magnitude scale due to its correlation with rupture parameters [15]. For converting M_s and m_b to M_w, the empirical relationships by Scordilis [16] is utilized whereas for conversions from M_d and M_l to M_w the study by Akkar et al. [17] is preferred. The conversion from M_s to M_w by Scodilis [16] is composed of a bilinear relationship that is given in Eq. (1).

$$M_w = 0.67(\pm 0.005)\, M_s + 2.07(\pm 0.03),\, 3.0 \leq M_s \leq 6.1 \tag{1.a}$$

$$M_w = 0.99(\pm 0.02)\, M_s + 0.08(\pm 0.13),\, 6.2 \leq M_s \leq 8.2 \tag{1.b}$$

Similarly, the relationship between m_b and M_w by Scordilis [16] is given in Eq. (2).

$$M_w = 0.85(\pm 0.04)\, m_b + 1.03(\pm 0.23),\, 3.5 \leq M_b \leq 6.2 \tag{2}$$

Akkar et al. [17] proposed linear relationships to convert M_d and M_l to M_w that are given in Eqs. (3) and (4) respectively.

$$M_w = 0.764(\pm 0.04)\, M_d + 1.379(\pm 0.2),\, 3.7 \leq M_d \leq 6.0 \tag{3}$$

$$M_w = 0.953(\pm 0.04)\, M_l + 0.422(\pm 0.21),\, 3.9 \leq M_l \leq 6.8 \tag{4}$$

For further analysis, the historical and instrumental catalogs are combined and converted to the M_w scale. The combined homogeneous catalog consists of 12737 earthquakes with magnitudes above $M_w \geq 4.0$.

5.1. Removing fore and after-shocks from the Catalog

One of the fundamental assumptions in PSHA is that earthquake occurrences verify Poisson model. On this basis of Poisson model, for a given threshold level the exceedance probabilities of any ground motion intensity measure (IM) is calculated. In order to apply Poisson model to earthquake occurrences, the fore and aftershocks need to be removed from the earthquake catalog. In this paper, we employed the window method by Gardner and Knopoff [18] to decluster the homogenous catalog. According to this method, all earthquakes in the catalog are regarded as potential fore/after shocks of a main shock and investigated within time and distance windows. In this study, the size of time and distance windows are determined according to the magnitude dependent relationship given by Gardner and Knopoff [18] as given in Eqs. (5) and (6). In order to eliminate the fore and aftershocks from the homogenous catalog we utilized ZMAP software.

$$R=10^{(0.1238M+0.983)} \tag{5}$$

- $t=10^{(0.032M+2.7389)}$ M≥6.5 $\tag{6a}$

- $t=10^{(0.5409M-0.547)}$ M<6.5 $\tag{6b}$

Figure 7 presents the declustered earthquake catalog properties in terms of cluster length in time and distance. As depicted in the figure, as magnitude increases temporal and spatial cluster lengths shift towards to the boundaries given by Gardner and Knopoff [18]. This observation complies with the magnitude effect on cluster sizes.
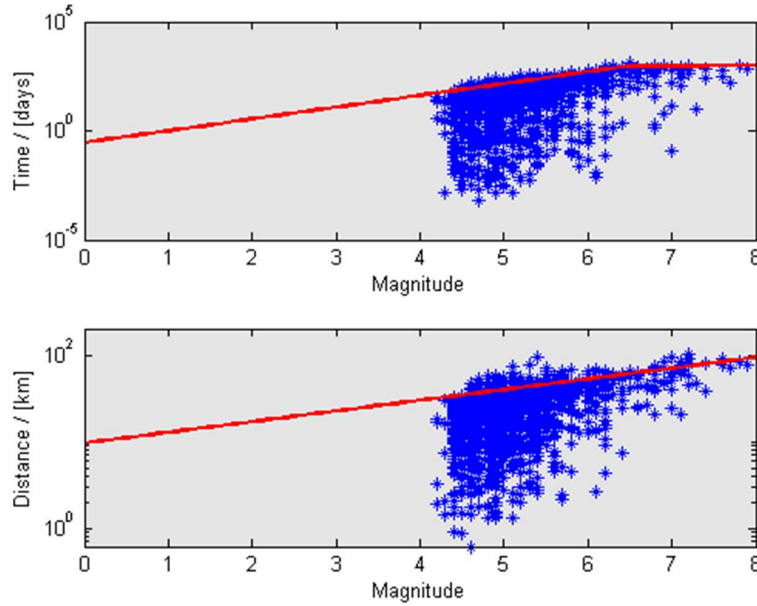

Figure 7. The cluster lengths in terms of time and distance

5.2. Completeness of the Catalog

Investigation on completeness of earthquake catalogs is very essential in seismic hazard analysis as it is directly linked to the magnitude recurrence relationships of area source models. The completeness of the catalog is investigated by two complementary methods proposed by Stepp [19] and Nasır et al. [20]. As these methods present the catalog completeness in different fashions, we take the advantage of both for the magnitude classes where decision on completeness was not straightforward. A single completeness analysis is conducted using the earthquakes that have occurred within the entire area source zones. According to the first method proposed by Stepp [19], the earthquakes in the catalog are first grouped in successive magnitude classes (e.g. M_w 4.3-4.7, M_w 4.8-5.2, M_w 5.3-5.7, M_w 5.8-6.2, M_w 6.3+). For each magnitude class, the mean earthquake rate is calculated for expanding time windows established from the last record towards the first one. As this method is based on stationarity of mean earthquake occurrence rate, for each magnitude class the variance of sample means is expected to have a trend similar to elapsed time in terms of years. The standard deviation of mean earthquake occurrence rate is calculated using Eq. (7).

$$\sigma_\lambda = \frac{\sqrt{\lambda}}{\sqrt{T}} \tag{7}$$

112

where, σ_λ is standard deviation, λ is mean and T is time. Similarly, σ_λ is expected to behave as $\sqrt{T}$. The σ_λ scatters for each magnitude class that are established with M_w 0.5 increments are presented in Figure 8.
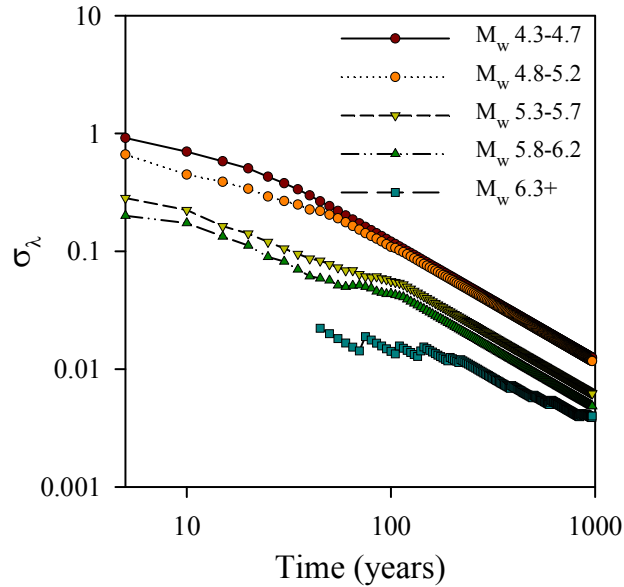
Figure 8. Standard deviation (σ_λ) scatters of the earthquake catalog for the combined area source zones

According to the method proposed by Nasır et al. [20], earthquakes in the catalog are first grouped in magnitude bins that are generally established with 0.5 magnitude increments. Then, for each magnitude bin the cumulative earthquake numbers are plotted against years. This plot is termed as "Temporal Course of Earthquake Frequency" (TCEF) plot by Nasır et al. [20]. Similar to the first method, the completeness of each magnitude class is determined according to the stationarity of the TCEF plots. Figure 9 illustrates the TCEF plots for the entire declustered earthquake catalog utilized in this study for the area of interest.

Figure 9. Temporal Course of Earthquake Frequency (TCEF) plots for each magnitude class of the declustered catalog that comprises of earthquakes within the combined area source zones.

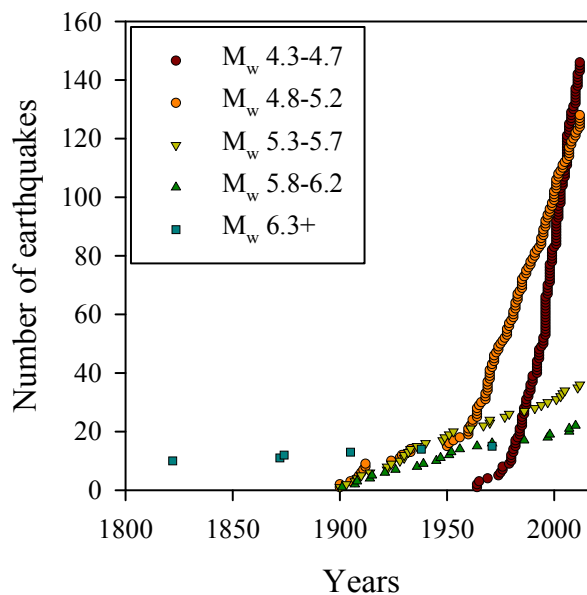Figure 8 and Figure 9 depict similar completeness intervals for the utilized earthquake catalog. By visual inspections, it is concluded that the catalog is incomplete for magnitudes $M_w \leq 4.2$ and complete after 1993, 1968, 1898, 1898 and 1823 for events with magnitudes $M_w \geq 4.3$, $M_w \geq 4.8$, $M_w \geq 5.3$, $M_w \geq 5.8$ and $M_w \geq 6.3$ respectively the completeness intervals of magnitude bins.

6. Characteristics of the Area Source Models

For each area source, the annual frequency of earthquakes with magnitudes exceeding a given magnitude (M) is calculated by the truncated exponential distribution (Eq. 8) given in McGuire [21].

$$n(M) = \nu_{M_{min}} \left[\frac{e^{(\beta M_{min} - \beta M)} - e^{(\beta M_{max} - \beta M_{min})}}{1 - e^{(\beta M_{max} - \beta M_{min})}} \right] \quad M_{min} \leq M \leq M_{max} \tag{8}$$

where, ν_{Mmin} is the annual rate of exceedance of events with magnitude M_{min}, and estimated by using the catalog information associated with background seismicity, β is the product of $\ln(10)$ and the "b" parameter in Richter [22] equation. For each area source, the maximum magnitude (M_{max}) is taken as either the magnitude of the biggest earthquake occurred in the region or maximum characteristic magnitude that the line sources within the boundary are able to produce. In this study, we employed the empirical relationship suggested by Wells and Coppersmith [23] to relate earthquake magnitudes to fault geometry and fault type. Activity rate of each area source is estimated by making use of the declustered homogenous catalog. We estimated magnitude recurrence parameters of each area source model in accordance with the Eq. (9) given by Weichert [24] for incomplete earthquake catalogs.

$$\nu_{M_{min}} = z_i \frac{\sum_i e^{-\beta M_i}}{\sum_i t_i e^{-\beta M_i}} \tag{9.a}$$

$$\frac{\sum_i t_i M_i e^{-\beta M_i}}{\sum_i t_i e^{-\beta M_i}} = \frac{\sum_i M_i z_i}{\sum_i z_i} \tag{9.b}$$

where, z_i is the number of the earthquakes with magnitude M_i, t_i is the duration that magnitude M_i is complete, and z_i is the number of earthquakes with magnitude M_i recorded in the duration t_i. The calculations related with the magnitude recurrence relationship of each area source model is conducted with the help of MATLAB based software generated by the first author. For exemplification purposes, the program window showing the exponential fit on magnitude-cumulative annual occurrence rate plot of Region 1 is presented in Figure 10. The magnitude recurrence parameters calculated for the area source models are tabulated in Table 1. As indicated in Table 1, area sources designated with IDs 1, 7, 8 and 10 represent interface and in-slab earthquakes while the rest stands for shallow crustal earthquakes.
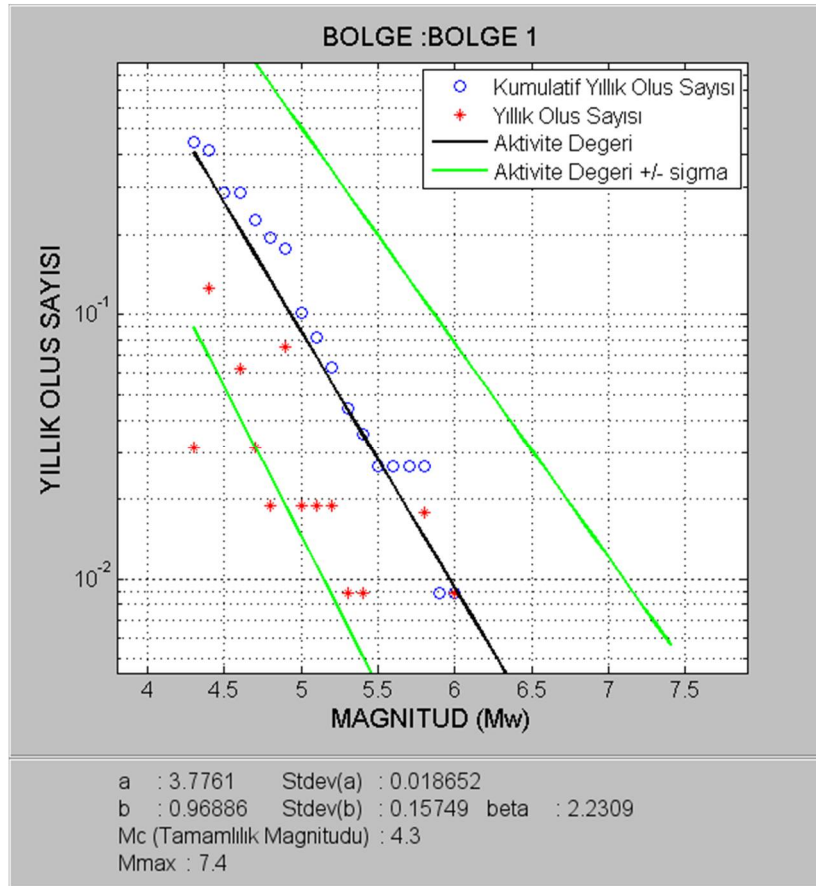
Figure 10. The window showing the magnitude recurrence relationship parameters of Region 1. The red stars correspond to the annual occurrence rates whereas blue circles represent the cumulative annual occurrence rates. The exponential fit is shown with black line together with the ± 1 standard deviations that are designated with green curves.

Table 1. Summary of the area source model characteristics

Area Source ID	M_{min}	M_{max}	β	ν_{min}	d_{max} (km)
1	4.3	7.4	2.230883	0.45546	35
2	4.4	7.5	2.121141	0.48931	20
3	4.3	7.3	2.835634	0.68537	20
4	4.4	7.4	2.063185	1.04104	20
5	4.3	7.3	2.476661	0.45878	20
6	4.3	7.4	2.259757	0.87368	20
7	4.3	7.6	2.302585	0.39890	50
8	4.5	6.5	2.302585	0.23817	50
9	4.3	7.7	2.451102	0.31892	20
10	4.4	6.9	2.018032	0.23050	35
11	4.3	7.1	2.766556	0.70230	20
12	4.4	7.2	2.302585	0.38019	20
13	4.5	6.6	2.508897	0.27860	20
14	4.3	6.9	2.248106	0.19670	20

7. The Ground Motion Prediction Equations (GMPEs) employed

In this study, we utilized a total of 6 GMPEs that are compatible with general seismotectonic structure in Turkey. The first group of the GMPEs are related to active shallow crust earthquakes whereas the second group corresponds to the interface and inslab earthquakes. In

the first group, Abrahamson and Silva [25], Campbell and Bozorgnia [26] and Chiou Youngs [27] prediction equations are utilized. In order to represent the inslab and interface earthquakes, we employed Atkinson and Boore [28], Zhao et al. [29] and Youngs [30] equations. Equal weight is given to the GMPEs for both active shallow crust earthquakes and subduction zone earthquakes. Table 2 presents general information on the utilized GMPEs.

Table 2. The GMPEs utilized for PSHA in this study

GMPE	Abb.[1]	Region	M_{min}[2] - M_{max}[3]	R_{type}[4] - R_{max}[5] (km)	Style of Faulting[7]
Abrahamson and Silva (2008)	AS08	Worldwide	M_w 5.0 - 8.5	R_{rup}[6], 200	SS, N, R
Campbell and Bozorgnia (2008)	CB08	Worldwide	M_w 4.0 - 8.5	R_{rup}[6], 200	SS, N, R
Chiou and Youngs (2008)	CY08	Worldwide	M_w 4.0 - 8.5	R_{rup}[6], 200	SS, N, R
Atkinson and Boore (2003)	AB03	Worldwide	M_w 5.5 - 8.3	R_{rup}[6], 550	Subduction
Zhao et al. (2006)	Z06	Japan	M_w 5.0 - 8.3	R_{rup}[6], 300	Subduction
Youngs (1997)	Yo97	Worldwide	M_w 5.0 - 8.2	R_{rup}[6], 550	Subduction

[1] Abbreviations of GMPEs; [2,3] M_{min} and M_{max} are minimum and maximum magnitude range of GMPEs; [4,5] R_{type} and R_{max} are source-to-site distance type and maximum distance range of GMPE, [6] R_{rup} is closest distance to rupture surface; [7] SS, N, R refer to strike-slip, normal and reverse faulting, respectively; [8] $V_{S,30}$ is average shear-wave velocity in the upper 30 m soil profile.

8. Seismic Hazard Maps for Adana

In the next step of the study, we conducted multi-site PSHA using EZ-FRISK software. The coordinates of each site is considered as the corner points of grids that are established with 0.1^0 x 0.1^0 cells. After conducting PSHA, bilinear interpolation is performed in order to generate iso-hazard maps.

Figure 11 shows the seismic hazard map of Adana in terms of PGA for 475 years and NEHRP C site condition. Similarly, the same plot for NEHRP D site condition is presented in Figure 12. As one can infer from the figures, the site class has a prominent effect on acceleration values. For the entire territory of Adana PGA values range between 0.23g and 0.37g when NEHRP C site class is assumed. On the other hand, the PGA values attain values between 0.26g and 0.41g if NEHRP D site class is considered.

Turkish Earthquake Code (TEC, 2007) provides effective peak accelerations 0.4g, 0.3g, 0.2g and 0.1g for seismic zones Zone I, II, III and IV respectively for a probability of exceedance of 10 % in 50 years (for a return period of T_R=475 years). The elastic design spectrum presented by TEC [2] only differs at corner periods for different site classes. In this sense, the effective peak accelerations given by TEC [2] correspond to the same PGA values for all site classes. Thus, a comparison is feasible between the proposed PGA values and the ones provided by seismic zonation map and TEC [2]. According to the seismic zonation map, the defined seismic zones for Adana Province is given in Figure 13. The immediate observation from these comparisons is the PGA values of the proposed maps do not vary significantly within the territory compared to those given by the current provisions. Moreover, the alignment of boundaries between different PGA values differ considerably. This observation is particularly pronounced in the eastern part of Adana where the proposed hazard maps suggest the highest PGA values. On the other hand, the seismic zonation map indicates that seismic hazard level attain the highest rate at Yumurtalık district. Although not given in this study, this site condition effect is also reflected in spectral accelerations of uniform hazard spectra calculated for several coordinates in Adana Province. This observation reveals the need for site amplification factors in design spectrum provided by TEC [2].
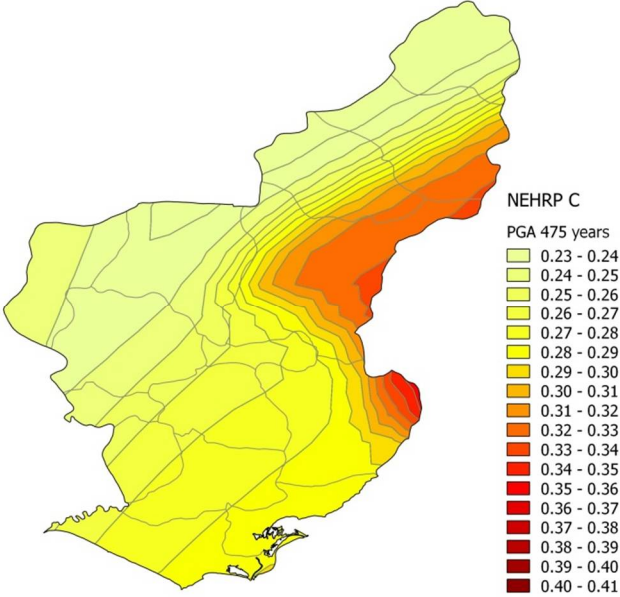
Figure 11. PGA hazard map of Adana for 475 year return period and NEHRP C site condition
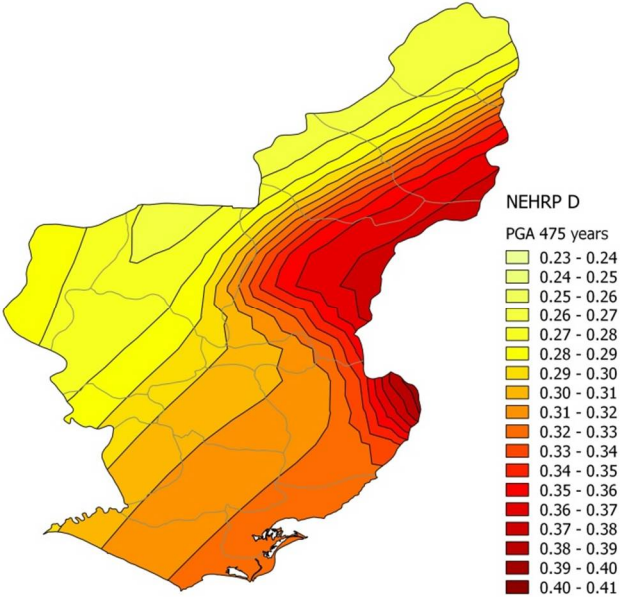

Figure 12. PGA hazard map of Adana for 475 year return period and NEHRP D site condition

Figure 13. Seismic zonation map of Adana (AFAD) [31]

9. Conclusions

In this paper, probabilistic seismic hazard analysis is performed for Adana province. The seismic hazard maps are presented in terms of PGA for 475 year return period and NEHRP C-D site conditions. The presented PGA hazard maps indicate that the seismic hazard in Adana is remarkably different compared to the PGA values given by the current seismic zonation map and Turkish Earthquake Code. The discrepancy in the distribution of seismic hazard as well as PGA levels raise several questions such as seismic reliability of new and existing buildings or site condition effect in the design spectrum ordinates. In this sense, it is believed that there is need for a revision in seismic zonation map and pertinent design spectra under the light of a comprehensive research.

References

[1] Afet ve Acil Durum Yönetimi Başkanlığı, AFAD, Aylık Deprem Raporu, Haziran, 2010.

[2] Turkish Eartquake Code, TEC. "Specification for Buildings to be built in Seismic Zones. Ankara, Turkey, Ministry of Public Works and Settlement, Government of Republic of Turkey, 2007.

[3] Woo, G., "Kernel Estimation Methods for Seismic Hazard Area Source Modeling," 86, 2, 353–362, 1996.

[4] Erdik, M., Biro, Y.A., Onur, T., Şeşetyan, K., and Birgoren, G., "Assessment of earthquake hazard in Turkey and neighboring regions" *Ann. di Geofis.*, vol. 42, no. 6, 1999.

[5] Özgül, N. ve Kozlu, H., Kozan-Feke (Doğu Toroslar) Yöresinin Stratigrafisi ve Yapısal Konumu İle İlgili Bulgular. TPJD Bülteni, 14 (1), 1-36. 2002

[6] Usta, D., Adana İli Jeolojik Özellikleri. MTA, Adana, pp 17, 2007. http://www.mta.gov.tr/v2.0/bolgeler/adana/bolgesel-jeoloji/jeoloji-adana.pdf, (accessed 21.01.2015)

[7] Rojay, B., Heimann, A., and Toprak, V., "Neotectonic and volcanic characteristics of the Karasu fault zone (Anatolia, Turkey): The transition zone between the Dead Sea transform and the East Anatolian fault zone," *Geodin. Acta*, 14, 197–212, 2001.

[8] Koçyiğit, A. and Özacar, A. A., "Extensional Neotectonic Regime through the NE Edge of the Outer Isparta Angle, SW Turkey : New Field and Seismic Data," *Turkish J. Earth Sci.*, 12, 67–90, 2003.

[9] Duman, T. Y., and Emre, O. The East Anatolian Fault: geometry, segmentation and jog characteristics. *Geological Society, London, Special Publications*, *372*(1), 495–529, 2013.

[10] Emre, Ö., Duman, T. Y., Özalp, S., Elmacı, H., Olgun, Ş and Şaroğlu F., "1:250,000 Scale Active Fault Map of Turkey", 2013.

[11] Global Earthquake Model, GEM. "Historical Earthquake Catalog", 2013.

[12] Turkelli, N., "Seismogenic zones in Eastern Turkey," *Geophys. Res. Lett.*, 30, 24, 8039, 2003.

[13] Vanacore, E. A., Taymaz, T., and Saygin, E., "Moho structure of the Anatolian Plate from receiver function analysis," *Geophys. J. Int.*, 193, 1, 329–337, 2013.

[14]. Kadirioglu, T. F., Kartal, R. F., Kılıç, T., Kalafat, D., Duman, T. Y., Özalp, S., Emre, Ö., "An Improved Earthquake Catalog (M≥4.0) For Turkey and Near Surrounding (1900-2012). Second European Conference on Earthquake Engineering and Seismology, İstanbul, 25-29 August, 2014.

[15] Ulusay, R., Tuncay, E., Sonmez, H., and Gokceoglu, C., "An attenuation relationship based on Turkish strong motion data and iso-acceleration map of Turkey," *Eng. Geol.*, 74, 3–4, 265–291, 2004.

[16] Scordilis, E. M., "Empirical Global Relations Converting Ms and mb to Moment Magnitude," *J. Seismol.*, 10, 2, 225–236, 2006.

[17] Akkar, S., Cagnan, Z., Yenier, E., Erdogan, O., Sandıkkaya, M. A., and Gülkan, P., "The Recently Compiled Turkish Strong-Motion Database : Preliminary Investigation for Seismological Parameters," *J. Seismol.*, 14, 457–479, 2010.

[18] Gardner, J. K. and Knopoff, L., "Bulletin of the Seismological Society of America," *Bull. Seismol. Soc. Am.*, 64, 5, 1363–1367, 1974.

[19] Stepp, J. C., "Analysis of Completeness of the Earthquake Sample in the Puget Sound Area and Its Effect on Statistical Estimates of Earthquake Hazard," in *Proceedings of the International Conference on Microzonation, Seattle, U.S.A*, 897–910, 1972.

[20] Nasir, A., Lenhardt, W., Hintersberger, E., and Decker, K., "Assessing the completeness of historical and instrumental earthquake data in Austria and the surrounding areas," *Austrian J. Earth Sci.*, 106, 1, 90–102, 2013.

[21] McGuire, R. K., "Seismic Hazard and Risk Analysis", Earthquake Engineering Research Institute Monograph, MNO-10, CA, 221p, 2004.

[22] Richter, C. F., Elementary Seismology. San Francisco, CA: W. H. Freeman, 1958.

[23] Wells, D. L. and Coppersmith, K. J., "New Empirical Relationships among Magnitude, Rupture Length , Rupture Width , Rupture Area , and Surface Displacement," *Bull. Seismol. Soc. Am.*, 84, 4, 974–1002, 1994.

[24] Weichert, D., "Estimation of the eartquake recurrence parameters for unequal observation periods for different magnitudes," *Bull. Seismol. Soc. Am.*, 70, 4, 1337–1346, 1980.

[25] Abrahamson, N. and Silva, W., "Summary of the Abrahamson & Silva NGA Ground-Motion Relations," *Earthq. Spectra*, 24, 1, 67–97, 2008.

[26] Campbell, K. W. and Bozorgnia, Y., "NGA Ground Motion Model for the Geometric Mean Horizontal Component of PGA, PGV, PGD and 5% Damped Linear Elastic Response Spectra for Periods Ranging from 0.01 to 10 s," *Earthq. Spectra*, 24, 1, 139–171, 2008.

[27] Chiou, B.-J. and Youngs, R. R., "An NGA Model for the Average Horizontal Component of Peak Ground Motion and Response Spectra," *Earthq. Spectra*, 24, 1, 173–215, 2008.

[28] Atkinson, G. M. and Boore, D. M., "Empirical ground-motion relations for subduction zone earth- quakes and their application to Cascadia and other regions". *Bull. Seismol. Soc. Am*, 93(4),1703–1729, 2003

[29] Zhao, J. X., "Attenuation Relations of Strong Ground Motion in Japan Using Site Classification Based on Predominant Period," *Bull. Seismol. Soc. Am.*, 96, 3, 898–913, Jun. 2006.

[30] Youngs, R. R., Chiou, S.-J., Silva, W. J., and Humphrey, J. R., "Strong ground motion attenuation relationships for Subduction Zone Earthquakes," *Seismol. Res. Lett.*, 68, 1, 58–73, 1997.

[31] Afet ve Acil Durum Yönetimi Başkanlığı, AFAD, Adana İli için Deprem Bölgeleri Haritası, http://www.deprem.gov.tr/sarbis/depbolge/adana1.gif, (accessed 19.02.2015).